Title

Tonoplast CBL–CIPK calcium signaling network regulates magnesium homeostasis in Arabidopsis

Journal

Proceedings of the National Academy of Sciences of the United States of America, 112(10)

ISSN

0027-8424

Authors

Tang, Ren-Jie
Zhao, Fu-Geng
Garcia, Veder J
et al.

Publication Date

2015-03-10

DOI

10.1073/pnas.1420944112

Peer reviewed

Tonoplast CBL–CIPK calcium signaling network regulates magnesium homeostasis in Arabidopsis

Ren-Jie Tang[a], Fu-Geng Zhao[b], Veder J. Garcia[a], Thomas J. Kleist[a], Lei Yang[b], Hong-Xia Zhang[c], and Sheng Luan[a,b,1]

[a]Department of Plant and Microbial Biology, University of California, Berkeley, CA 94720; [b]Nanjing University–Nanjing Forestry University Joint Institute for Plant Molecular Biology, State Key Laboratory for Pharmaceutical Biotechnology, College of Life Sciences, Nanjing University, Nanjing 210093, China; and [c]National Key Laboratory of Plant Molecular Genetics, Institute of Plant Physiology and Ecology, Shanghai Institutes for Biological Sciences, Chinese Academy of Sciences, Shanghai 200032, China

Edited by Natasha V. Raikhel, Center for Plant Cell Biology, Riverside, CA, and approved January 7, 2015 (received for review November 4, 2014)

Although Mg^{2+} is essential for a myriad of cellular processes, high levels of Mg^{2+} in the environment, such as those found in serpentine soils, become toxic to plants. In this study, we identified two calcineurin B-like (CBL) proteins, CBL2 and CBL3, as key regulators for plant growth under high-Mg conditions. The *Arabidopsis* mutant lacking both CBL2 and CBL3 displayed severe growth retardation in the presence of excess Mg^{2+}, implying elevated Mg^{2+} toxicity in these plants. Unexpectedly, the *cbl2 cbl3* mutant plants retained lower Mg content than wild-type plants under either normal or high-Mg conditions, suggesting that CBL2 and CBL3 may be required for vacuolar Mg^{2+} sequestration. Indeed, patch-clamp analysis showed that the *cbl2 cbl3* mutant exhibited reduced Mg^{2+} influx into the vacuole. We further identified four CBL-interacting protein kinases (CIPKs), CIPK3, -9, -23, and -26, as functionally overlapping components downstream of CBL2/3 in the signaling pathway that facilitates Mg^{2+} homeostasis. The *cipk3 cipk9 cipk23 cipk26* quadruple mutant, like the *cbl2 cbl3* double mutant, was hypersensitive to high-Mg conditions; furthermore, CIPK3/9/23/26 physically interacted with CBL2/3 at the vacuolar membrane. Our results thus provide evidence that CBL2/3 and CIPK3/9/23/26 constitute a multivalent interacting network that regulates the vacuolar sequestration of Mg^{2+}, thereby protecting plants from Mg^{2+} toxicity.

magnesium toxicity | calcium sensor | vacuole | magnesium transport

Plants absorb essential mineral nutrients from the soil and translocate them to different organs for specific physiological processes. Most of these minerals are in the ionic forms and require a wide array of transporters to move them across the cell membranes and sort them into subcellular compartments (1). Although plants rely on a sufficient supply of mineral nutrients for proper growth and development, an excess of minerals often causes toxicity to plant cells. To adapt to the constantly changing availability of minerals in the environment, plants have evolved mechanisms that enhance ion uptake under low-nutrient conditions and sequester excessive ions in the vacuole when external levels are high. Such mechanisms enable plant cells to maintain a steady level of each nutrient ion, namely, ionic homeostasis. At the molecular level, this homeostasis entails the coordinated functions of a large number of regulatory molecules that constitute elaborate signaling networks to control the affinities and activities of numerous ion transporters. In these signaling networks, Ca^{2+} serves as a central messenger (2). A number of external ionic stresses can evoke stimulus-specific cellular Ca signals that are represented by the distinct spatiotemporal patterns of Ca^{2+} fluxes between cytosol and Ca^{2+} stores (3, 4). These "Ca^{2+} signatures" can be detected and relayed into diverse downstream signaling events by plant Ca^{2+}-sensor proteins that manifest conformational changes upon binding Ca^{2+} and subsequently regulate the function of target proteins (5–7).

Calcineurin B-like (CBL) proteins are a group of Ca^{2+} sensors that physically and functionally interact with a family of plant-specific protein kinases designated as "CBL-interacting protein kinases" (CIPKs) (8). Interaction between CBLs and CIPKs is mediated by the regulatory C-terminal region of CIPKs and is required for full activation of the kinase activity (9–11). Although CIPKs appear to be soluble in the cytosol, CBL proteins are largely associated with the cellular membranes through their N-terminal motifs that are subject to lipid modifications (12). Some CBLs, such as CBL1, -4, -5, and -9, are anchored to the plasma membrane through myristoylation and acylation at their N-terminal region (13). Other CBLs including, CBL2, -3, and -6, are localized to the vacuolar membrane via the N-terminal tonoplast targeting sequence that contains multiple cysteine residues subject to S-acylation (14, 15). It has been suggested that the dynamic localization of CIPKs is determined by their specific CBL partners, resulting in alternative CBL–CIPK complexes at either the plasma membrane or the tonoplast (16–18).

Growing evidence has highlighted the CBL–CIPK regulatory pathways in plant responses to environmental stresses in general and ionic stresses in particular (19). In the Ca^{2+}-dependent salt overly sensitive (SOS) pathway, the Ca sensor CBL4/SOS3 (20) and the protein kinase CIPK24/SOS2 (21) form a functional module to regulate the Na^+/H^+ exchanger SOS1 at the plasma membrane, thus facilitating Na^+ extrusion under salt stress (22). Another CBL protein, CBL10/SCaBP8, was identified as a shoot-specific partner of CIPK24 in salt stress adaptation (16, 23, 24). In response to limited K^+ supply, the Ca sensors CBL1 and CBL9 positively regulate CIPK23 and recruit the kinase to the plasma membrane, which in turn activates the K^+ channel AKT1 for optimal K^+ nutrition (25–27). Interestingly, the CBL1/9–CIPK23 module also regulates nitrate (NO_3^-) uptake and sensing processes by phosphorylating the dual-affinity NO_3^- transporter CHL1 (28). A recent study shows that CIPK23, in

Significance

Plant growth requires a balanced supply of mineral nutrients. However, the availability of minerals varies constantly in the environment. How do plants adapt to low or high levels of minerals in the soil? The answer to this question holds the key to sustainable crop production. Mg is an essential macronutrient for plants, but high levels of Mg^{2+} can become toxic. This study uncovered a regulatory mechanism, consisting of two calcineurin B-like (CBL) Ca sensors partnering with four CBL-interacting protein kinases (CIPKs) forming a CBL–CIPK network that allows plant cells to sequester the extra Mg^{2+} into vacuoles, thereby protecting plant cells from high-Mg toxicity. To our knowledge, this report is the first that describes such a signaling mechanism for regulation of Mg homeostasis.

Author contributions: R.-J.T. and S.L. designed research; R.-J.T., F.-G.Z., and V.J.G. performed research; L.Y. and H.-X.Z. contributed new reagents/analytic tools; R.-J.T., F.-G.Z., T.J.K., L.Y., and S.L. analyzed data; and R.-J.T. and S.L. wrote the paper.

The authors declare no conflict of interest.

This article is a PNAS Direct Submission.

See Commentary on page 2931.

[1]To whom correspondence should be addressed. Email: sluan@berkeley.edu.

This article contains supporting information online at www.pnas.org/lookup/suppl/doi:10.1073/pnas.1420944112/-/DCSupplemental.

complex with CBL1 or CBL9, could trigger the opening of the S-type anion channel SLAC1 or SLAH3 through its phosphorylation in a Ca-dependent manner (29).

Ionic homeostasis is regulated mainly by ion transport across the plasma membrane and vacuolar membrane (tonoplast). Although CBL–CIPK signaling modules are well recognized as playing a critical role in the transport of several minerals across the plasma membrane, very little is known about the possible function of vacuolar CBL–CIPK complexes. Our recent work revealed a highly redundant role for tonoplasts CBL2 and CBL3 in plant development and ion homeostasis that is correlated with the regulation of vacuolar H^+-ATPase (V-ATPase) activity (14). In this study, we describe a novel function of CBL2 and CBL3 in the regulation of Mg^{2+} homeostasis through a V-ATPase–independent pathway in *Arabidopsis*. Downstream of CBL2 and CBL3 are four functionally redundant CIPKs that are recruited to the tonoplast by interacting with CBL2 and CBL3. Our results thus build a CBL–CIPK network at the tonoplast that regulates vacuolar sequestration to detoxify excessive Mg^{2+} in plant cells.

Results

A Null Mutant Lacking Both CBL2 and CBL3 Exhibits V-ATPase–Dependent and –Independent Defects in Ionic Homeostasis. We previously constructed a *cbl2 cbl3* double mutant and characterized its phenotype during different developmental stages as well as under multiple ionic stress conditions. Although transfer DNA (T-DNA) insertions were located in the 5′ UTR of *CBL2* and *CBL3*, both lines represented knockout alleles because full-length transcripts were not detectable (14). To corroborate the double knockout at the protein level, we performed Western blot analysis using a polyclonal antibody raised against the CBL3 protein. Because of the high homology between CBL2 and CBL3, this antibody was also cross-reactive with CBL2 protein, although with a considerably lower affinity. Nevertheless, the overall protein level of CBL2 and CBL3 was undetectable in the double-mutant background (Fig. 1*A*), ensuring that *cbl2 cbl3* is indeed a null mutant lacking both CBL2 and CBL3 protein.

Our previous work suggested that CBL2 and CBL3 modulate V-ATPase activity that in turn controls plant growth and ion homeostasis (14). Further analysis of the *cbl2 cbl3* double mutant identified defects that are absent in the V-ATPase–null mutant, suggesting that CBL2 and CBL3 may regulate both V-ATPase–dependent and other, V-ATPase–independent, processes. Although they grow normally on the 1/6 Murashige and Skoog (MS) medium (Fig. 1*B*), both *cbl2 cbl3* and *vha-a2 a3* mutant (a tonoplast V-ATPase–null allele) plants were hypersensitive to excessive Ca^{2+} (Fig. 1*C*). However, the *cbl2 cbl3* mutant displayed unique sensitivity to high levels of external Mg^{2+} not shared by *vha-a2 a3* (Fig. 1*D*). Measurements of seedling fresh weight confirmed a severe growth inhibition by 4 mM $MgCl_2$ in the *cbl2 cbl3* mutant, but not in the *vha-a2 a3* mutant, as compared with wild-type plants (Fig. 1*E*). To validate that the hypersensitivity of *cbl2 cbl3* to $MgCl_2$ is specifically attributable to Mg^{2+} but not to the anion, we replaced $MgCl_2$ with other Mg^{2+} salts in our assay and found that *cbl2 cbl3* was sensitive to all the Mg^{2+} salts tested (Fig. S1 *A–E*). High levels of Mg^{2+} did not appear to affect seed germination but exerted the toxicity on postgermination growth (Fig. S1*F*). These results uncovered a novel physiological role of CBL2 and CBL3 in the context of Mg^{2+} homeostasis that is independent of V-ATPase function.

CBL2 and CBL3 Function Redundantly in High-Mg Tolerance in *Arabidopsis*. To conduct detailed assessment of Mg^{2+} sensitivity of *cbl2 cbl3*, we used full-strength MS medium supplemented with a broad range of Mg^{2+}concentrations for growth assays. After growing on MS medium modified with a reduced level of Mg^{2+} (1 mM) for 2 wk, the stature of *cbl2 cbl3* mutant plants was comparable to that of wild-type plants (Fig. 2*A*). Adding 5 mM

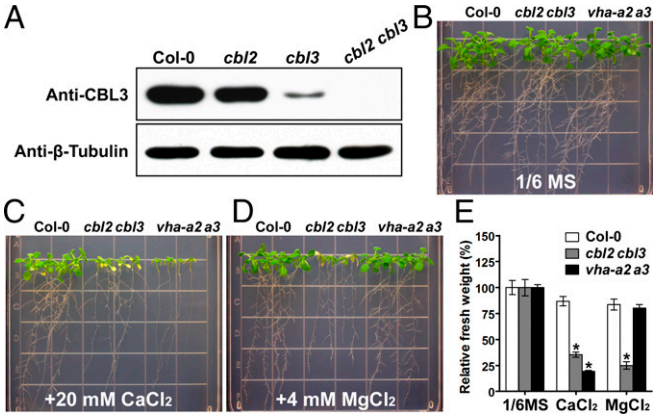

Fig. 1. The *cbl2 cbl3* double-knockout mutant showed V-ATPase–dependent and –independent ionic sensitivity. (*A*) Western blot analysis of wild-type Col-0, the *cbl2* or *cbl3* single mutant, and the *cbl2 cbl3* double mutant. CBL2 and CBL3 protein levels were analyzed by immunoblotting using a CBL3 antibody. The amount of β-tubulin was determined in parallel as a loading control. (*B–D*) Growth phenotype of wild-type Col-0 and *cbl2 cbl3* and *vha-a2 a3* mutant plants under different ionic stress conditions. Four-day-old seedlings were transferred onto 1/6 MS medium (*B*) or 1/6 MS medium supplemented with 20 mM $CaCl_2$ (*C*) or 4 mM $MgCl_2$ (*D*). Photographs were taken on the 18th day after transfer. (*E*) Fresh weight of seedlings on the 18th day after transfer. Data are presented as the mean ± SE of four replicate experiments. Asterisks indicate statistically significant differences compared with the Col-0 (Student's *t* test, $*P < 0.05$).

or 10 mM Mg^{2+} into MS medium did not affect the growth of wild-type plants but drastically reduced the stature of the *cbl2 cbl3* mutant (Fig. 2 *B* and *C*). Further increases of Mg^{2+} (up to 31.5 mM) in the medium inhibited the growth of wild-type plants as well, whereas *cbl2 cbl3* plants could hardly survive under the same conditions (Fig. 2 *D–F*). Quantitative analysis of root length (Fig. 2*G*) and fresh weight (Fig. 2*H*) indicated that, compared with the wild-type plants, *cbl2 cbl3* mutants displayed more severe growth retardation as affected by external Mg^{2+} in a dosage-dependent manner.

To dissect the contribution of CBL2 and CBL3 to high-Mg tolerance, we further examined the growth phenotype of *cbl2* and *cbl3* single mutants on high-Mg medium. In contrast to the hypersensitivity of the double mutant, single mutants did not show significant differences from wild type under high-Mg conditions (Fig. S2). Moreover, expression of either CBL2 or CBL3 under the control of the *CBL2* native promoter rescued the growth phenotype of the double mutant under high-Mg conditions (Fig. S3). Taken together, these results demonstrate that CBL2 and CBL3 function redundantly in high-Mg tolerance in *Arabidopsis*.

The *cbl2 cbl3* Mutant Accumulates Less Mg and Is Defective in Vacuolar Mg^{2+} Conductance. To explore the possible mechanism underlying increased Mg^{2+} sensitivity in the *cbl2 cbl3* mutant, we decided to measure the Mg content in Col-0 and *cbl2 cbl3* plants. Because Ca and Mg often antagonize each other in their uptake and transport (30), we also measured the Ca content in the same plants. Compared with Col-0 plants, *cbl2 cbl3* mutants consistently retained less Mg in either the root or the shoot (Fig. 3 *A* and *B*). The difference in shoot Mg content was most striking when 20 mM Mg^{2+} was added to the growth medium (Fig. 3*B*). Consistent with Mg–Ca antagonism, the Ca content in both wild-type and *cbl2 cbl3* mutant plants was evidently lower when high concentrations of Mg^{2+} were included in the medium. Although Ca content in the roots was comparable in Col-0 and *cbl2 cbl3* plants (Fig. 3*C*), the shoot Ca content was significantly lower in *cbl2 cbl3* than in Col-0 plants (Fig. 3*D*) under all external Mg^{2+}

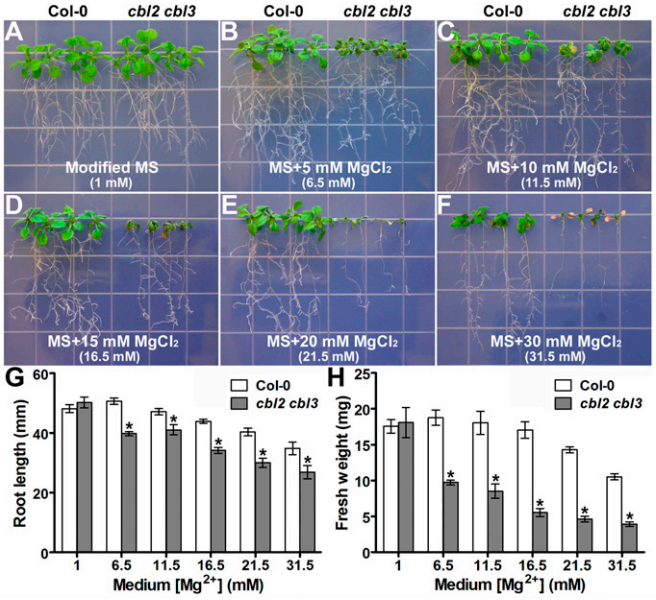

Fig. 2. *cbl2 cbl3* mutant plants were hypersensitive to external Mg^{2+} in a dosage-dependent manner. (*A–F*) Growth phenotype of Col-0 and *cbl2 cbl3* under different concentrations of external $MgCl_2$. Four-day-old Col-0 and *cbl2 cbl3* seedlings were transferred onto modified MS medium with a reduced level of Mg^{2+} (*A*) or MS supplemented with 5 mM (*B*), 10 mM (*C*), 15 mM (*D*), 20 mM (*E*), or 30 mM (*F*) $MgCl_2$. The final Mg^{2+} concentration of each panel is given in parentheses. Photographs were taken on the 14th day after the transfer. (*G*) Length of primary roots of wild-type Col-0 and *cbl2 cbl3* plants on the 14th day after the transfer. (*H*) Fresh weight of Col-0 and *cbl2 cbl3* seedlings on the 14th day after the transfer. Data are presented as the mean ± SE of four replicate experiments. Asterisks indicate statistically significant differences between Col-0 and *cbl2 cbl3* plants (Student's *t* test, $*P < 0.05$).

concentrations, suggesting that partition of both Mg and Ca are altered in the *cbl2 cbl3* mutant.

The balance between Mg^{2+} and Ca^{2+} has long been considered to be a critical factor for plant growth (31, 32). Because *cbl2 cbl3* mutant plants are defective in the accumulation of both Ca and Mg, particularly under high-Mg conditions, the Mg-sensitive phenotype may be a result of Mg toxicity or Ca deficiency. Thus, we tested the growth phenotype of *cbl2 cbl3* on media with variable Mg^{2+}/Ca^{2+} ratios. Under 6 mM or 12 mM Mg^{2+}, both wild-type and double-mutant plants grew poorly when external Ca^{2+} levels were low, but increasing Ca^{2+} levels dramatically improved plant growth (Fig. S4), supporting the general notion of Mg–Ca antagonism. However, mutant plants consistently performed more poorly than the wild-type plants under all conditions, supporting the idea that CBL2 and CBL3 are required for Ca–Mg homeostasis. Interestingly, with a normal Mg^{2+} concentration (0.75 mM) in MS medium, even an extremely low level (0.03 mM) of Ca^{2+} supported plant growth to the same extent in wild-type and *cbl2 cbl3* plants (Fig. S4*I*), suggesting that high Mg^{2+}, rather than Ca^{2+} deficiency, is the primary factor that caused growth defects in the *cbl2 cbl3* mutant. We thus focused on Mg homeostasis in further analysis.

Because CBL2 and CBL3 are targeted specifically to the tonoplast, and the double mutant is sensitive to high-Mg levels but contains much less Mg, we reasoned that the vacuolar sequestration of Mg^{2+} might be reduced in the *cbl2 cbl3* mutant, resulting in toxicity to plants. We tested this hypothesis by measuring the outward Mg^{2+} currents across the tonoplast (Mg^{2+} influx from the cytosol into the vacuole) using the patch-clamp technique. Intact vacuoles from mesophyll cells of wild-type plants were isolated and clamped between −40 and +100 mV with a 0.6-s duration and in 20-mV increments (Fig. 4*A*). In the whole-vacuole mode, outward Mg^{2+} currents were detected at positive test voltages, which consisted of an instantaneous component and a slow time-dependent component (Fig. 4*B*). Current amplitude increased in response to a higher Mg^{2+} concentration on the cytoplasmic side of the membrane (Fig. S5*A*). A plot of the steady-state current densities at three different cytosolic $MgCl_2$ concentrations showed that Mg^{2+} was transported into the vacuole across the tonoplast in a dosage-dependent manner (Fig. S5*B*). To ensure that the observed currents were generated by Mg^{2+} influx and not by the efflux of anions, we used different forms of Mg^{2+} in the bath and pipette solutions. The current amplitude did not respond to changes in the anion species (Fig. S5*C*). Moreover, several anion channel blockers had no effect on the detected currents (Fig. S5*D*), indicating that the current resulted from cation (Mg^{2+}) movement across the vacuolar membrane. Under the same experimental condition, vacuoles from *cbl2 cbl3* mutants displayed significantly reduced outward currents compared with those from wild-type plants (Fig. 4*C*). At a test voltage of +100 mV, the current amplitude observed in *cbl2 cbl3* vacuoles was less than 50% of that in the wild-type plants (Fig. 4*D*). These electrophysiological experiments suggested that Mg^{2+} influx into the vacuolar lumen was severely impaired in the *cbl2 cbl3* plants, leading to reduced Mg content and more severe growth retardation in the double mutant under high-Mg conditions.

It is generally believed that the pH gradient across the tonoplast results in a negative membrane potential against cation influx into the vacuole. However, that potential might be altered rapidly by changes in ionic accumulation under various conditions. For instance, Mg^{2+} accumulation in the cytosol under high-Mg stress can depolarize the tonoplast potential and result in more positive values, thereby activating the cation influx channel and Mg^{2+} sequestration into the vacuole.

CIPK3,-9, -23, and -26 Are Required for High-Mg Tolerance in *Arabidopsis*. It has been established that CBLs and their interacting CIPKs work together as obligate partners in the signaling pathway. To identify the CIPK(s) downstream of CBL2/3 in the regulation of high-Mg tolerance, we screened all *cipk* single mutants under Mg^{2+} stress conditions to identify those with a phenotype similar to that of *cbl2 cbl3*. However, none of these single mutants appeared to grow differently from the wild type under high-Mg conditions, implying that CIPKs are functionally redundant in this physiological process. We then mined the public microarray database to identify CIPK genes whose expression is regulated by high-Mg stress. This analysis identified the *CIPK9* gene as significantly up-regulated in response to high Mg^{2+} (33). Indeed, using a quantitative real-time PCR (qRT-PCR) assay, we found that the expression level of *CIPK9* increased steadily after the onset of high-Mg treatment and reached a fourfold induction at the 24 h (Fig. S6*A*). Expression

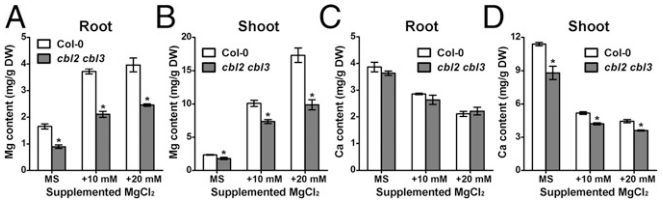

Fig. 3. Mg and Ca content in the *cbl2 cbl3* mutant. (*A*) Mg content in the root under different Mg^{2+} regimes. (*B*) Mg content in the shoot under different Mg^{2+} regimes. (*C*) Ca content in the root under different Mg^{2+} regimes. (*D*) Ca content in the shoot under different Mg^{2+} regimes. Data are presented as the mean ± SE of triplicate experiments. Asterisks indicate statistically significant differences between Col-0 and *cbl2 cbl3* plants (Student's *t* test, $*P < 0.05$).

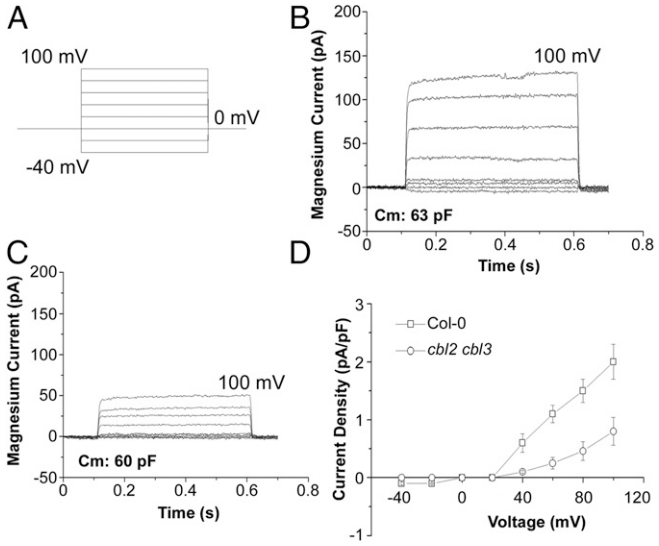

Fig. 4. Whole-vacuole Mg^{2+} currents were reduced in the vacuoles from *cbl2 cbl3* double-mutant plants. (*A*) Recording protocol. From a holding potential of 0 mV, a series of test voltages between −40 and +100 mV was applied in 20-mV steps. Corresponding whole-vacuole currents were recorded under 20 mM $MgCl_2$. (*B*) Whole-vacuole Mg^{2+} current density traces of a representative wild-type vacuole. The membrane capacitance was 63 pF. (*C*) Whole-vacuole Mg^{2+} current density traces of a representative *cbl2 cbl3* vacuole. The membrane capacitance was 60 pF. (*D*) Current–voltage relationship derived from whole-vacuole Mg^{2+} currents across the tonoplast from wild-type (□, $n = 20$) and *cbl2 cbl3* mutant (○, $n = 26$) plants.

of *CIPK23*, *CIPK26*, and *CBL3* was marginally increased by high Mg^{2+} (Fig. S6*A*).

Phylogenetic analysis indicated that CIPK23, -3, and -26 are close homologs of CIPK9 that can be grouped into one clade in the *Arabidopsis* CIPK family (Fig. S6*B*). Because none of the single mutants showed any discernible difference in terms of Mg^{2+} sensitivity compared with the wild type (Fig. S7*D*), we constructed double mutants between *cipk9* and *cipk23* and between *cipk3* and *cipk26*, and ultimately a quadruple mutant *cipk3 cipk9 cipk23 cipk26* (hereafter, "*cipk3/9/23/26*") was generated by crossing the two double mutants (Fig. S7 *A* and *B*). Although the two double mutants *cipk3/26* and *cipk9/23* exhibited only subtle sensitivity to high levels of external Mg^{2+} (Fig. S7 *C* and *E*), the quadruple mutant *cipk3/9/23/26* could fully phenocopy the Mg^{2+} hypersensitivity in the *cbl2 cbl3* mutant under either moderate or high levels of external Mg^{2+} (Fig. 5 *A*–*D*). Furthermore, the *cipk3/9/23/26* mutant also showed an ionic profile similar to that of *cbl2 cbl3*; namely, both Mg and Ca were lower than in wild-type plants under either normal or high-Mg stress conditions (Fig. 5 *E* and *F*). These results suggest that CIPK3, -9, -23, and -26 may be functional partners of CBL2/3 in controlling Mg^{2+} homeostasis and high-Mg tolerance in *Arabidopsis*.

CBL2/3 Interact with and Recruit CIPK3/9/23/26 to the Tonoplast. Genetic evidence supports the hypothesis that CIPK3/9/23/26 and CBL2/3 may function in the same pathway in the control of Mg^{2+} homeostasis and high-Mg tolerance. Because formation of CBL–CIPK complexes is the hallmark of the CBL–CIPK signaling mechanism, we examined whether CBL2 and CBL3 interact physically with these CIPKs. Using the yeast two-hybrid assay, we found that CIPK3/9/23/26 indeed interact directly with CBL2 and CBL3 (Fig. 6*A*). As expected, CIPK26 lacking the C-terminal CBL-interacting domain (NAF domain) did not interact with CBL2 or CBL3 (Fig. 6*A*). To determine if they interact in plant cells, we used the bimolecular fluorescence complementation (BiFC) assay, in which CBL2 and CBL3 were fused to the C-terminal fragment of YFP (YC), and each of the CIPKs was fused to the N-terminal fragment of YFP (YN). When CBL2-YC was cotransformed with each of the YN-CIPKs into the *Arabidopsis* mesophyll protoplasts, the YFP signals produced by all CBL2–CIPK interaction pairs were clearly observed at the vacuolar membrane (Fig. 6*B*). As a negative control, deletion of the NAF domain from CIPK26 abolished the interaction with CBL2 (Fig. 6*B*). Repeating the same BiFC procedure with CBL3-YC in combination with each individual YN-CIPK produced a similar result; namely, CBL3 and each CIPK also interacted and such interaction took place at the tonoplast. Taken together, these data suggest that both CBL2 and CBL3 recruit CIPK3/9/23/26 to the tonoplast where these functionally overlapping CBL–CIPK complexes may regulate the transport proteins responsible for vacuolar partitioning of Mg^{2+}.

Discussion

The Ca sensor CBLs and their interacting protein kinases, the CIPKs, constitute a complex signaling network that enables plants to adapt to environmental changes. Regulation of membrane transport processes appears to be an emerging theme in the function of CBL–CIPK signaling machinery (19). Extensive evidence supports the idea that CBL–CIPK modules control the activity of ionic transport across the plasma membrane, but little is known about CBL–CIPK function in the control of vacuolar transport despite the predominant role of large vacuoles in osmotic adjustments and nutrient storage-supply in plant cells. In this report, we have described a novel function of CBL2 and CBL3 in regulating intracellular Mg^{2+} homeostasis, which is independent of V-ATPase. Furthermore, we identified four downstream kinases, CIPK3, -9, -23, and -26, that work together with CBL2 and CBL3 in the same pathway for regulation of Mg^{2+} transport across the tonoplast.

High concentrations of environmental Mg^{2+} could be detrimental to plant growth (Fig. 2) (33). However, because Mg^{2+} is a macronutrient required for plant growth, its toxic effect at high

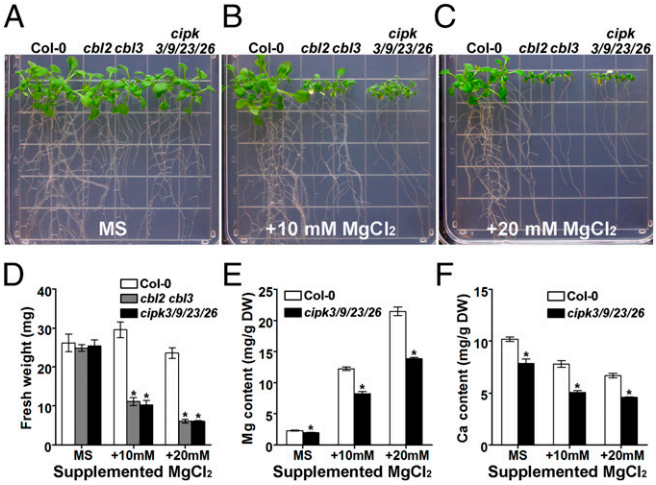

Fig. 5. The *cipk3/9/23/26* quadruple mutant was hypersensitive to high-Mg stress. (*A*–*C*) Phenotype analysis of Col-0, *cbl2 cbl3*, and *cipk3/9/23/26* seedlings under high-Mg conditions. Four-day-old seedlings grown on MS medium were transferred onto MS medium (*A*) or MS medium supplemented with 10 mM (*B*) or 20 mM (*C*) $MgCl_2$. Photographs were taken on the 14th day after the transfer. (*D*) Fresh weight of the seedlings on the 14th day after the transfer. Data shown are the mean ± SE of four replicate experiments. (*E* and *F*) Mg (*E*) and Ca (*F*) content of Col-0 and *cipk3/9/23/26* seedlings under different Mg^{2+} regimes. Data are presented as the mean ± SE of triplicate experiments. Asterisks indicate statistically significant differences compared with wild-type Col-0 (Student's *t* test, $*P < 0.05$).

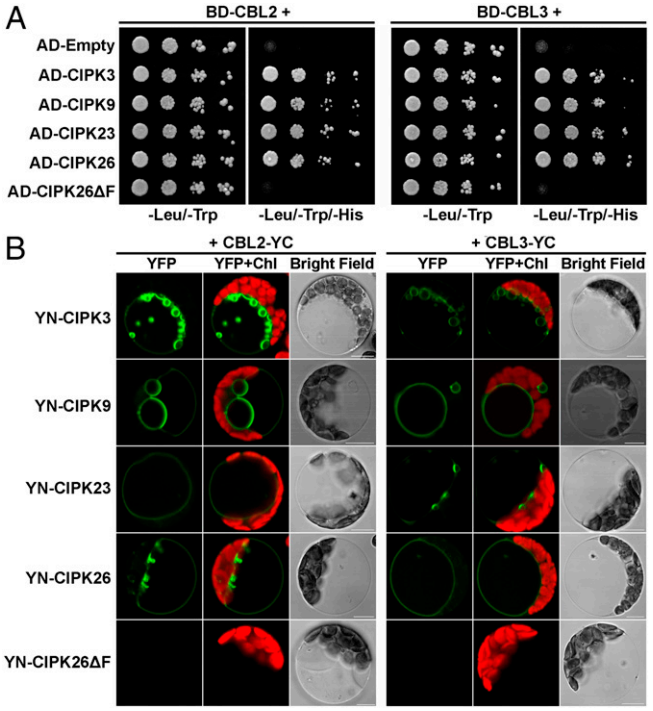

Fig. 6. Interaction of CBL2/3 and CIPK3/9/23/26 at the tonoplast. (*A*) Yeast two-hybrid assay of the interactions between CBL2/3 and different CIPKs. Yeast AH109 cells were cotransformed with various combinations of BD- and AD-fusion constructs as indicated above and on the left of each panel, respectively. CIPK26ΔF represents CIPK26 lacking NAF domain. Serial decimal dilutions of corresponding yeast cells were spotted onto selective SD medium without leucine and tryptophan as a control or onto the selective SD medium lacking leucine, tryptophan, and histidine for monitoring growth. Photographs were taken after cultivation for 3 d at 30 °C. (*B*) BiFC analysis of CBL2/3 and CIPK3/9/23/26 interaction in plant protoplasts. The CBL2-YC or CBL3-YC fusion construct, in combination with various YN-fusion constructs as indicated in the left column, was transformed into *Arabidopsis* mesophyll protoplasts. The YFP signal and chloroplast autofluorescence (Chl) were imaged under a Zeiss confocal microscope as green and red, respectively. (Scale bar: 10 μm.)

levels and the mechanisms underlying this toxicity have been largely overlooked. In the present study, we identified two Ca sensors and their interacting kinases as required for the regulation of Mg^{2+} tolerance, opening up a new avenue for exploring molecular mechanisms of Mg^{2+} homeostasis and tolerance in plants. Consistent with the observation that Ca^{2+}–Mg^{2+} balance is important for plant growth (31, 32), the *cbl2 cbl3* double mutant was extremely sensitive to external Mg^{2+} when the Ca^{2+} level in the medium was low. In contrast, high levels of Ca^{2+} in the medium could partially alleviate the severe growth defect of *cbl2 cbl3* under high-Mg stress (Fig. S4). The Ca^{2+} dependence of high-Mg sensitivity is not unique to the *cbl2 cbl3* mutant but is also observed in the wild type. Therefore, the general toxic effect of high Mg^{2+} in plants could be attributed, at least in part, to impaired Ca^{2+} homeostasis. Consistent with this idea, Ca^{2+} uptake was found to be considerably inhibited by excessive Mg^{2+} (Fig. 3), as Ca^{2+} and Mg^{2+} might compete for the same transporters in the plasma membrane (30). Such Mg^{2+}/Ca^{2+} balance is reminiscent of the Na^+/K^+ balance critical for growth under high-Na conditions (34), emphasizing the importance of homeostatic balance among the mineral nutrients for plant growth.

Being not only a nutrient but also a second messenger, Ca^{2+} is essential for plant growth as well as for adaption to environmental changes. Stimulus-induced Ca^{2+} signals in response to various abiotic and biotic stresses have been well documented in plant cells (4). For instance, Na^+ stress elicits a cell type-specific Ca^{2+} signal (35) that can be propagated systemically and transmitted from root to the shoot (36). It is tempting to speculate that excess Mg^{2+} would also trigger a rapid change in the cytoplasmic Ca^{2+} level through an unknown mechanism. The tonoplast-localized Ca^{2+} sensors CBL2 and CBL3 probably are capable of decoding the Ca^{2+} signature in response to high-Mg stress. Upon sensing the specific Ca signal, CBL2 and CBL3 regulate the downstream protein kinases CIPK3, -9, -23, and -26, likely by modifying their activities and their subcellular localization. The tonoplast-localized CBL2/3–CIPK3/9/23/26 complexes further regulate target proteins that transport Mg^{2+} into the vacuoles, protecting plant cells from toxic levels of Mg^{2+}. Several lines of evidence support this working model. First, in contrast to a relatively stable level of Mg^{2+} at around 0.2–0.4 mM in the cytosol (37), plant vacuoles can accumulate a large amount of Mg^{2+}, reaching as high as 80 mM in the leaves of *Arabidopsis* plants fed with high-Mg solutions (38). This suggests that upon high-Mg stress excess Mg would go to the vacuole, leaving the cytosolic level rather constant. The high-Mg–sensitive phenotype of *cbl2 cbl3* and *cipk3/9/23/26* thus could be the result of these mutants having a defective pathway for vacuolar Mg^{2+} sequestration, leading to a more toxic level of Mg^{2+} in the cytoplasm. Second, using electrophysiological analysis in the whole-vacuole mode, we identified an outward Mg^{2+} current across the tonoplast that represents Mg^{2+} influx into the vacuolar lumen. Interestingly, the *cbl2 cbl3* double mutant exhibited a significantly smaller current for vacuolar Mg^{2+} influx than did the wild type, indicating that the CBL2/3-mediated pathway indeed regulates vacuolar Mg^{2+} sequestration. Third, CBL2/3 physically interacted with and recruited downstream kinases CIPK3/9/23/26 to the tonoplast. This specific interaction at the vacuolar membrane would facilitate fast relays of Ca^{2+} signals to local targets and provide a molecular basis for the signaling specificity of the CBL–CIPK regulatory module.

Further work will be directed to identifying the transporter/channel serving as the target of CBL2/3–CIPK3/9/23/26 at the tonoplast. Relevant to this goal, some earlier studies suggested that Mg^{2+} influx from the cytosol into the vacuole could be mediated by Mg^{2+}/H^+ antiporters (39), and a single protein, AtMHX, was identified as fulfilling such a role in *Arabidopsis* (40). However, we found that the knockout mutant *mhx* was not sensitive to high external Mg^{2+} (Fig. S8), arguing against a role for AtMHX in detoxifying excessive cytosolic Mg^{2+}. Another group of tonoplast-localized Mg transporters, MGT2 and MGT3, are implicated in Mg^{2+} partitioning into mesophyll vacuoles in *Arabidopsis* (38). Our analysis of the *mgt2 mgt3* double mutant failed to reveal a high Mg-sensitive phenotype (Fig. S8), suggesting that MGT2 and MGT3 may not account for vacuolar Mg transport associated with Mg tolerance. Identifying the elusive Mg transporter(s) that mediates vacuolar Mg^{2+} influx will be a critical next step toward understanding the mechanism for CBL–CIPK–regulated high-Mg tolerance in plants.

Methods

Plant Materials and Growth Conditions. *Arabidopsis thaliana* Columbia (Col) ecotype was used in this study. The *cbl2 cbl3* and *vha-a2 a3* double mutants were described in previous studies (14, 41). The T-DNA insertion mutants *cipk3* (SAIL_409A04), *cipk9* (SALK_058629), *cipk23* (SALK_036154), *cipk26* (GK-703D04), *mhx* (SALK_068941), *mgt2* (SALK_006797), and *mgt3* (GK-592B07) were obtained from the *Arabidopsis* Biological Resource Center or the European *Arabidopsis* Stock Centre. Mutants with multiple gene-knockout events were constructed by genetic crosses, and homozygous mutant plants were screened from F2 or F3 progeny and identified by genomic PCR using primers listed in *SI Methods*.

For on-plate growth assays, wild-type and mutant seeds were sterilized with 0.5% sodium hypochlorite for 5 min, washed three times, and sown on MS medium solidified with 0.8% phytoagar (Caisson Labs). The plates were kept at 4 °C for 2 d and then were positioned vertically at 22 °C. Four-day-old seedlings were then transferred onto various agarose-solidified media as indicated in the figures and were grown under 60–90 $\mu mol \cdot m^{-2} \cdot s^{-1}$ light intensity with a 12-h light/12-h dark photoperiod.

Measurements of Mg and Ca Content. One-week-old *Arabidopsis* seedlings were transferred onto MS medium supplemented with 0, 10, or 20 mM $MgCl_2$. Ion contents were measured in wild-type and mutant plants on the ninth day after seedling transfer. Seedlings were collected and pooled into roots and shoots. The samples were dried for 48 h at 80 °C, milled to fine powder, weighed, and digested with ultrapure HNO_3 (Sigma-Aldrich). Mg^{2+} and Ca^{2+} concentrations were determined using inductively coupled plasma optical emission spectroscopy (PerkinElmer).

Electrophysiological Procedure. Whole-vacuole Mg currents were recorded using the standard patch-clamp procedure essentially as described by Beyhl et al. (42). Patch pipettes were prepared from borosilicate glass capillaries (Sutter Instrument Co.) with a P-97 puller (Sutter Instrument Co.) and were fire-polished to a final tip resistance of 5–6 MΩ. Whole-vacuole recordings were performed with the Axon Multiclamp 700B Amplifier (Molecular Devices). The pipette solution contained 20 mM $MgCl_2$, 1 mM $CaCl_2$, 10 mM Mes-bis-Tris, propane (Mes-BTP, pH 6.0). The bath solution contained 20 mM $MgCl_2$, 6.7 mM EGTA, 5.864 mM $CaCl_2$, 10 mM Mes-BTP (pH 7.2). The osmolarity of the pipette and bath solution was adjusted to 550 mOsm and 500 mOsm, respectively, by the addition of D-sorbitol. Recordings were initiated 10 min after break-in. Digital low-pass filtering of currents was performed at a cutoff frequency of 2.9 kHz. According to the convention of electrical recording of ionic fluxes across an endomembrane (43), positive currents correspond to cations moving from the cytoplasmic side into the vacuolar lumen. Steady-state currents were calculated by averaging the last 100 ms of each current trace. Raw currents were normalized into current densities (pA/pF) by taking into consideration the tonoplast capacitance of each vacuole. Current–voltage relationships were obtained by plotting current densities against the applied test voltages.

BiFC Assay. To generate BiFC constructs, the coding sequence of CBL2 and CBL3 without the stop codon was in-frame cloned into the pUC-PYCE(M) vector, and the coding sequence of each CIPK was subcloned into the pUC-SPYNE(R)173 vector (17). For transient expression, different combinations of these plasmids were transformed into *Arabidopsis* mesophyll protoplasts by a PEG-mediated transfection procedure (44). After the transfected protoplasts were incubated at 24 °C for 16 h, YFP and chlorophyll signals were imaged by the LSM510 META confocal laser scanning microscope (Carl Zeiss). The excitation wavelength for YFP was 514 nm, and the emission wavelength was between 535 and 600 nm.

ACKNOWLEDGMENTS. We thank the *Arabidopsis* Biological Resource Center and the European *Arabidopsis* Stock Centre for providing *Arabidopsis thaliana* seed stocks. This work was supported by National Science Foundation Grants MCB-0723931 and ISO-1339239 (to S.L.) and National Natural Science Foundation of China Grants 31270303 (to F.-G.Z.) and 31171169 (to H.-X.Z.).

1. Ward JM, Mäser P, Schroeder JI (2009) Plant ion channels: Gene families, physiology, and functional genomics analyses. *Annu Rev Physiol* 71:59–82.
2. Dodd AN, Kudla J, Sanders D (2010) The language of calcium signaling. *Annu Rev Plant Biol* 61:593–620.
3. Hetherington AM, Brownlee C (2004) The generation of $Ca^{(2+)}$ signals in plants. *Annu Rev Plant Biol* 55:401–427.
4. McAinsh MR, Pittman JK (2009) Shaping the calcium signature. *New Phytol* 181(2): 275–294.
5. Luan S, Kudla J, Rodriguez-Concepcion M, Yalovsky S, Gruissem W (2002) Calmodulins and calcineurin B-like proteins: Calcium sensors for specific signal response coupling in plants. *Plant Cell* 14(Suppl):S389–S400.
6. Harper JF, Breton G, Harmon A (2004) Decoding $Ca^{(2+)}$ signals through plant protein kinases. *Annu Rev Plant Biol* 55:263–288.
7. DeFalco TA, Bender KW, Snedden WA (2010) Breaking the code: Ca^{2+} sensors in plant signalling. *Biochem J* 425(1):27–40.
8. Shi J, et al. (1999) Novel protein kinases associated with calcineurin B-like calcium sensors in Arabidopsis. *Plant Cell* 11(12):2393–2405.
9. Albrecht V, Ritz O, Linder S, Harter K, Kudla J (2001) The NAF domain defines a novel protein-protein interaction module conserved in Ca^{2+}-regulated kinases. *EMBO J* 20(5):1051–1063.
10. Guo Y, Halfter U, Ishitani M, Zhu JK (2001) Molecular characterization of functional domains in the protein kinase SOS2 that is required for plant salt tolerance. *Plant Cell* 13(6):1383–1400.
11. Chaves-Sanjuan A, et al. (2014) Structural basis of the regulatory mechanism of the plant CIPK family of protein kinases controlling ion homeostasis and abiotic stress. *Proc Natl Acad Sci USA* 111(42):E4532–E4541.
12. Batistic O, Waadt R, Steinhorst L, Held K, Kudla J (2010) CBL-mediated targeting of CIPKs facilitates the decoding of calcium signals emanating from distinct cellular stores. *Plant J* 61(2):211–222.
13. Batistic O, Sorek N, Schültke S, Yalovsky S, Kudla J (2008) Dual fatty acyl modification determines the localization and plasma membrane targeting of CBL/CIPK Ca^{2+} signaling complexes in Arabidopsis. *Plant Cell* 20(5):1346–1362.
14. Tang RJ, et al. (2012) Tonoplast calcium sensors CBL2 and CBL3 control plant growth and ion homeostasis through regulating V-ATPase activity in Arabidopsis. *Cell Res* 22(12):1650–1665.
15. Batistič O, et al. (2012) S-acylation-dependent association of the calcium sensor CBL2 with the vacuolar membrane is essential for proper abscisic acid responses. *Cell Res* 22(7):1155–1168.
16. Kim BG, et al. (2007) The calcium sensor CBL10 mediates salt tolerance by regulating ion homeostasis in Arabidopsis. *Plant J* 52(3):473–484.
17. Waadt R, et al. (2008) Multicolor bimolecular fluorescence complementation reveals simultaneous formation of alternative CBL/CIPK complexes in planta. *Plant J* 56(3):505–516.
18. Schlücking K, et al. (2013) A new β-estradiol-inducible vector set that facilitates easy construction and efficient expression of transgenes reveals CBL3-dependent cytoplasm to tonoplast translocation of CIPK5. *Mol Plant* 6(6):1814–1829.
19. Luan S (2009) The CBL-CIPK network in plant calcium signaling. *Trends Plant Sci* 14(1):37–42.
20. Liu J, Zhu JK (1998) A calcium sensor homolog required for plant salt tolerance. *Science* 280(5371):1943–1945.
21. Liu J, Ishitani M, Halfter U, Kim CS, Zhu JK (2000) The *Arabidopsis thaliana* SOS2 gene encodes a protein kinase that is required for salt tolerance. *Proc Natl Acad Sci USA* 97(7):3730–3734.
22. Qiu QS, Guo Y, Dietrich MA, Schumaker KS, Zhu JK (2002) Regulation of SOS1, a plasma membrane Na^+/H^+ exchanger in *Arabidopsis thaliana*, by SOS2 and SOS3. *Proc Natl Acad Sci USA* 99(12):8436–8441.
23. Quan R, et al. (2007) SCABP8/CBL10, a putative calcium sensor, interacts with the protein kinase SOS2 to protect Arabidopsis shoots from salt stress. *Plant Cell* 19(4):1415–1431.
24. Tang RJ, et al. (2014) Poplar calcineurin B-like proteins PtCBL10A and PtCBL10B regulate shoot salt tolerance through interaction with PtSOS2 in the vacuolar membrane. *Plant Cell Environ* 37(3):573–588.
25. Xu J, et al. (2006) A protein kinase, interacting with two calcineurin B-like proteins, regulates K^+ transporter AKT1 in Arabidopsis. *Cell* 125(7):1347–1360.
26. Li L, Kim BG, Cheong YH, Pandey GK, Luan S (2006) A $Ca^{(2)+}$ signaling pathway regulates a $K^{(+)}$ channel for low-K response in Arabidopsis. *Proc Natl Acad Sci USA* 103(33):12625–12630.
27. Cheong YH, et al. (2007) Two calcineurin B-like calcium sensors, interacting with protein kinase CIPK23, regulate leaf transpiration and root potassium uptake in Arabidopsis. *Plant J* 52(2):223–239.
28. Ho CH, Lin SH, Hu HC, Tsay YF (2009) CHL1 functions as a nitrate sensor in plants. *Cell* 138(6):1184–1194.
29. Maierhofer T, et al. (2014) Site- and kinase-specific phosphorylation-mediated activation of SLAC1, a guard cell anion channel stimulated by abscisic acid. *Sci Signal* 7(342):ra86.
30. Yermiyahu U, Nir S, Ben-Hayyim G, Kafkafi U (1994) Quantitative competition of calcium with sodium or magnesium for sorption sites on plasma membrane vesicles of melon (*Cucumis melo* L.) root cells. *J Membr Biol* 138(1):55–63.
31. Bradshaw HD, Jr (2005) Mutations in CAX1 produce phenotypes characteristic of plants tolerant to serpentine soils. *New Phytol* 167(1):81–88.
32. Yamanaka T, et al. (2010) MCA1 and MCA2 that mediate Ca^{2+} uptake have distinct and overlapping roles in Arabidopsis. *Plant Physiol* 152(3):1284–1296.
33. Visscher AM, et al. (2010) Growth performance and root transcriptome remodeling of Arabidopsis in response to Mars-like levels of magnesium sulfate. *PLoS ONE* 5(8):e12348.
34. Maathuis FJM, Amtmann A (1999) K^+ nutrition and Na^+ toxicity: The basis of cellular K^+/Na^+ ratios. *Ann Bot (Lond)* 84(2):123–133.
35. Knight H, Trewavas AJ, Knight MR (1997) Calcium signalling in *Arabidopsis thaliana* responding to drought and salinity. *Plant J* 12(5):1067–1078.
36. Choi WG, Toyota M, Kim SH, Hilleary R, Gilroy S (2014) Salt stress-induced Ca^{2+} waves are associated with rapid, long-distance root-to-shoot signaling in plants. *Proc Natl Acad Sci USA* 111(17):6497–6502.
37. Hermans C, Conn SJ, Chen J, Xiao Q, Verbruggen N (2013) An update on magnesium homeostasis mechanisms in plants. *Metallomics* 5(9):1170–1183.
38. Conn SJ, et al. (2011) Magnesium transporters, MGT2/MRS2-1 and MGT3/MRS2-5, are important for magnesium partitioning within *Arabidopsis thaliana* mesophyll vacuoles. *New Phytol* 190(3):583–594.
39. Amalou Z, Gibrat R, Brugidou C, Trouslot P, d'Auzac J (1992) Evidence for an amiloride-inhibited $Mg^{2+}/2H^+$ antiporter in lutoid (vacuolar) vesicles from latex of *Hevea brasiliensis*. *Plant Physiol* 100(1):255–260.
40. Shaul O, et al. (1999) Cloning and characterization of a novel $Mg^{(2+)}/H^{(+)}$ exchanger. *EMBO J* 18(14):3973–3980.
41. Krebs M, et al. (2010) Arabidopsis V-ATPase activity at the tonoplast is required for efficient nutrient storage but not for sodium accumulation. *Proc Natl Acad Sci USA* 107(7):3251–3256.
42. Beyhl D, et al. (2009) The *fou2* mutation in the major vacuolar cation channel TPC1 confers tolerance to inhibitory luminal calcium. *Plant J* 58(5):715–723.
43. Bertl A, et al. (1992) Electrical measurements on endomembranes. *Science* 258(5084): 873–874.
44. Yoo SD, Cho YH, Sheen J (2007) Arabidopsis mesophyll protoplasts: A versatile cell system for transient gene expression analysis. *Nat Protoc* 2(7):1565–1572.